01 Jan 2006

Transverse-Earthquake Induced Deformations of a Bridge Approach Embankment in the New Madrid Seismic Zone

Wanxing Liu

Richard Wesley Stephenson
Missouri University of Science and Technology

Ronaldo Luna
Missouri University of Science and Technology, rluna@mst.edu

Recommended Citation

W. Liu et al., "Transverse-Earthquake Induced Deformations of a Bridge Approach Embankment in the New Madrid Seismic Zone," *Proceedings of the GeoShanghai Conference (2006, Jun. 6-8, Shanghai, China): Ground Modification and Seismic Mitigation*, American Society of Civil Engineers (ASCE), Jan 2006.
The definitive version is available at https://doi.org/10.1061/40864(196)53

Earthquake-Induced Deformations Of A Bridge Approach Embankment In The New Madrid Seismic Zone

W.X. Liu[1], R.W. Stephenson[2] and R. Luna[3]

Abstract

It is predicted that strong earthquakes larger than M7.0 may occur within next 50 years in the New Madrid Seismic Zone (NMSZ), the location of three of the most powerful earthquakes in United States history. Large displacements may occur during strong earthquakes to make an embankment fail or lose its function. The hyperbolic stress-strain model with Masing rules was modified to account for strength and stiffness reduction due to the effective confining pressure change. Byrne model was combined with the hyperbolic model to calculate the pore water pressure caused by seismic shaking. This modified hyperbolic model was implemented into the FLAC computer code and calibrated against the 1971 Upper San Fernando Dam failure. Then it was applied to study the seismically induced deformation of an approach embankment to Bridge A1466 in the NMSZ near Hayti, Missouri.

Introduction

The permanent deformations that occur to an approach embankment of a bridge during an earthquake event are very important. If large deformations occur, the bridge has “failed” since it cannot be used for its design purpose, which is to access the bridge. Quantifying earthquake-induced deformation analyses is one of the biggest challenges in geotechnical earthquake engineering.

Newmark (1965), Makdisi and Seed (1978), Rathje and Bray (1999), and Lin

[1] Geostructural Group, Schnabel Engineering, 510 East Gay Street, West Chester, PA 19380, USA; PH (1-610) 696-6066; FAX (1-610) 696-7771; email: wliu@schnabel-eng.com

[2] Department of Civil, Architectural & Environmental Engineering, 127 Butler-Carlton Hall, 1870 Miner Circle, University of Missouri-Rolla, Rolla, MO 65409-0300 USA; PH (1-573) 341-6549; FAX (1-573) 341-4729; email: stephens@umr.edu

[3] Department of Civil, Architectural & Environmental Engineering, 130 Butler-Carlton Hall, 1870 Miner Circle, University of Missouri-Rolla, Rolla, MO 65409-0300 USA; PH (1-573) 341-4484; FAX (1-573) 341-4729; email: rluna@umr.edu

and Hynes (1998) developed empirical methods to estimate the soil displacement under cyclic loading. Finn et al. (1986, 1999) and Wu (1998, 2001) proposed and modified the nonlinear hysteretic stress-strain soil model combined with Martin-Finn-Seed approach (Martin et al. 1975). Some elastic-plastic models using Biot's coupled equations, including DYNAFLOW (Prevost 1981), DYSAC2 (Muraleetharan et al. 1988), and SWANDYNE4 (Zienkiewicz et al. 1990a, 1990b), were developed for pore pressure and deformation calculation. Each approach has its advantages and limitations. Due to the complexity of the problem, the objective of these analyses is focused on predicting general deformation patterns and approximate estimates of displacement magnitudes. In this study the hyperbolic model was modified, calibrated and implemented into FLAC to analyze the seismic performance of the approach embankment at Bridge Site A1466.

Modified Hyperbolic/Byrne Model

There is a built-in model, Finn model, in FLAC. It is the standard Mohr-Coulomb model with increments of deformation taken from the volumetric strain, predicted by Byrne model, every time a "cycle" is detected. This crude model does not consider the shear modulus degradation and damping variation with shear strain and the shear strength and maximum shear modulus loss due to the effective confining pressure change. In order to consider all these effects, the hyperbolic model using Masing rules (1926) was modified and implemented into FLAC.

The stress strain relationship for Masing rules are shown in Figure 1. Since this model uses a tangent elastic modulus, no residual or plastic volume deformation remains after the loading. In order to calculate the residual or plastic volume deformation, the empirical Byrne relations between irrecoverable volumetric strain and cyclic shear strain were incorporated into the hyperbolic model. It is expressed by the following equation (Byrne, 1991)

$$\frac{\Delta\varepsilon_{vd}}{\gamma} = C_1 \exp(-C_2(\frac{\varepsilon_{vd}}{\gamma})) \tag{1}$$

where $C_1 = 8.7(N_1)_{60}^{-1.25}$ and $C_2 = \dfrac{0.4}{C_1}$. The shear strain γ in the two equations is defined as peak-to-peak shear strain.

Shear modulus, bulk modulus, and shear strength are all controlled by the effective confining stress. Seed and Idriss (1970) proposed the relationship between the shear modulus and the confining pressure as follows:

$$G_{\max} = 1000 K_{2\max} \left(\sigma'_m\right)^{0.5} \tag{2}$$

where $K_{2\max}$ and σ'_m are shear modulus number and mean effective confining stress, respectively.

In the modified hyperbolic model, the maximum shear modulus, shear strength, and bulk modulus are reduced due to the excess pore water pressure. They are updated in the each element by the following equations:

$$G_0 = G_{\max}\left(\frac{\sigma'_m}{\sigma'_{m0}}\right)^{0.5} \tag{3}$$

$$\tau_0 = \tau_{\max}\left(\frac{\sigma'_m}{\sigma'_{m0}}\right) \tag{4}$$

$$k = \left(2G_{\max}(1+v)\right)/(3(1-2v)) \tag{5}$$

where G_0, τ_0, σ'_{m0}, σ'_m, and v are the updated initial shear modulus, the updated initial shear strength, initial effective mean confining stress, the updated effective mean confining stress, and Poisson's ratio, respectively.

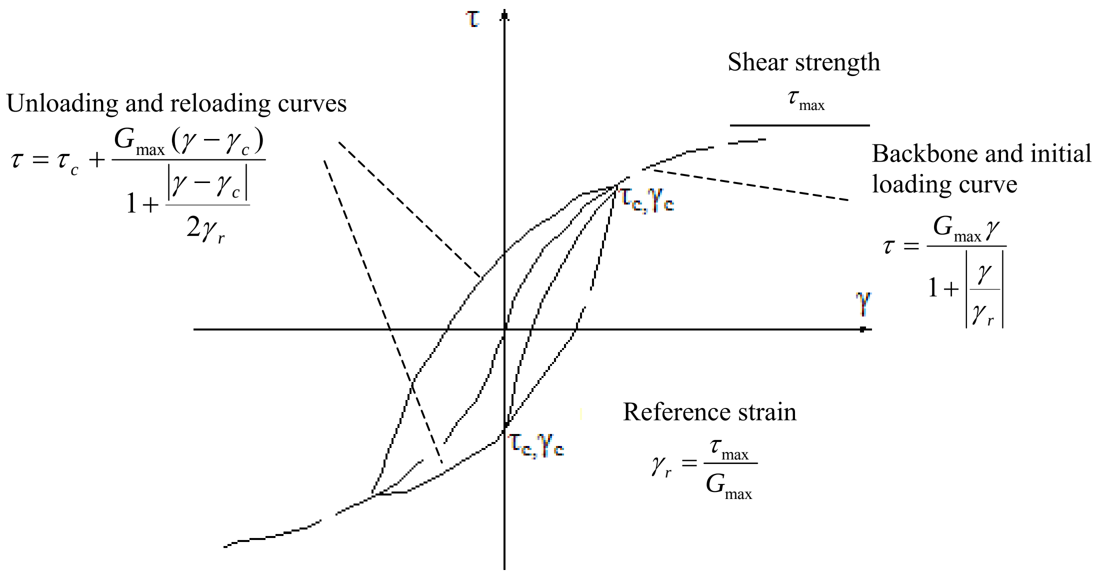

Figure 1. Hyperbolic stress-strain relationship

Calibration of the Modified Hyperbolic Model

To confirm the validity of implemented hyperbolic model, it was calibrated against the 1971 Upper San Fernando Dam failure, located in southern California. This hydraulic fill dam was constructed on about 15 to 18 m of alluvium overlying bedrock. A 5.5-meter-high rolled fill section was placed on the upstream portion of the hydraulic fill, leaving a 30.5m wide bench on the downstream slope. The slopes of this dam are 2.5:1. The representative cross section is shown in Figure 2.

The ground motion (EERC 73-2) developed by Seed et al. (1973) was used. SPT tests were performed at the site during April and May 1971, as reported by Harder et al. (1986). Soil properties are correlated from SPT N values and estimated from cross-hole seismic surveys for the dynamic analysis.

The computed deformations and measured displacements (Serf et al. 1976) at the end of the earthquake using the implemented hyperbolic model are shown in Figure 3.

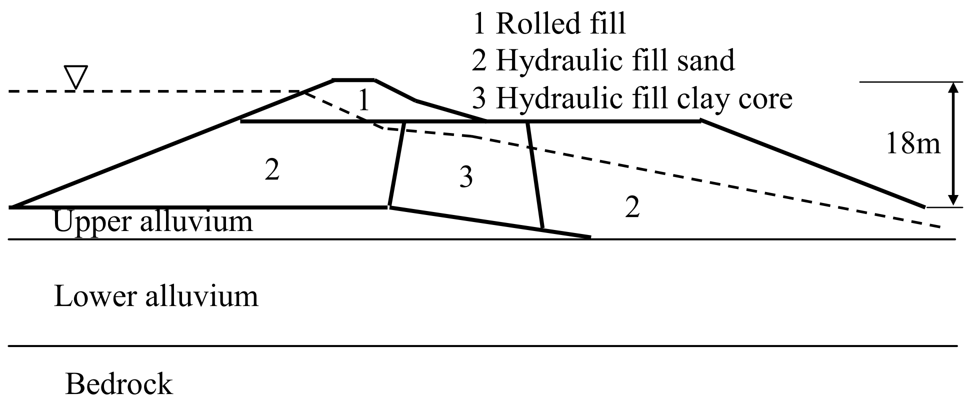

Figure 2. Soil profile of Upper San Fernando Dam (Seed et al., 1973)

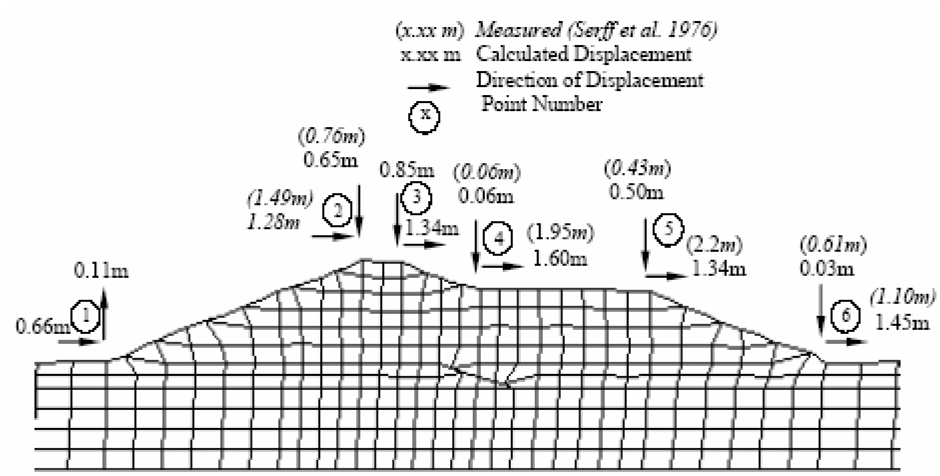

Figure 3. Deformed mesh after earthquake using modified hyperbolic model

Figure 4 illustrates the computed displacements using both Finn and the modified hyperbolic models and measured displacements along the embankment profile. It was observed that the deformed pattern is almost same.

The calculated, measured, and modified deformations at different locations using both Finn and modified hyperbolic models are shown in Table 2. It is seen that the calculated displacements using the Finn model are lower than the measured values (Seed et al. 1973), but the calculated displacements using the hyperbolic model agree well with the measured values (Serff et al. 1976). The measured and modified measured displacements are close only at point 2 and totally different at point 6. The reason may be that the modified measured values are inferred from the numerical and empirical analysis. Compared with the original measured values, the hyperbolic model can give very good results. Therefore, the hyperbolic model can provide reasonable results and better understanding of the deformation of earth structures during earthquakes.

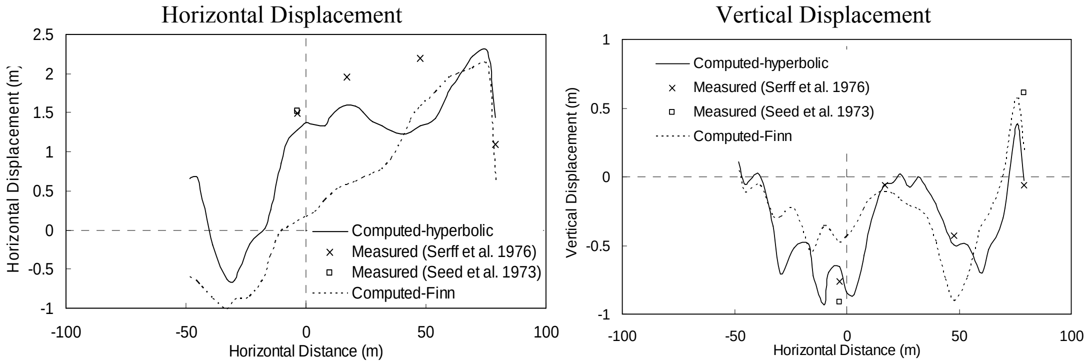

Figure 4. Displacements along embankment profile

Table 2. The calculated, measured and modified measured deformations

Position	Finn model		Hyperbolic model		Modified from measured (Serff et al. 1976)		Measured (Seed et al. 1973)	
	x	y	x	y	x	y	x	y
Point 1	-0.61	0.05	0.66	0.11	-	-		
Point 2	0.11	-0.47	1.28	-0.65	1.49	-0.76	1.52	-0.91
Point 3	0.23	-0.37	1.34	-0.85	-	-	-	-
Point 4	0.57	-0.11	1.60	-0.06	1.95	-0.06	-	-
Point 5	1.59	-0.90	1.34	-0.50	2.2	-0.43	-	-
Point 6	0.63	0.19	1.45	-0.03	1.1	-0.06	-	0.61

Application of the Modeling Technique to NMSZ Highway Embankments

To understand the performance of the embankment during an earthquake, the calibrated hyperbolic model was applied to determine the deformations in the transverse cross section of the approach embankment to Bridge A1466 in the NMSZ. To reduce the boundary effect and study the liquefaction potential of foundation soils, the depth of 37 m of foundation soils was included in the embankment system as shown in Figure 5.

The bottom boundary was fixed. Free-field boundaries (Seed et al. 1975) were applied to the vertical sides of the model to minimize wave reflections and achieve free-field conditions. Ground motions were input at the bottom of the model. Ground motions were obtained from the site response analysis accounting for high confining pressure effect (Liu, 2005). A total of five ground motions at M7.0 were used for this study to understand the general behavior of the embankment-foundation soil system. Index, permeability, and triaxial tests were conducted on the samples taken from the embankment and subgrade soils. The shear wave velocity was measured using SCPT, cross-hole and SASW test procedures.

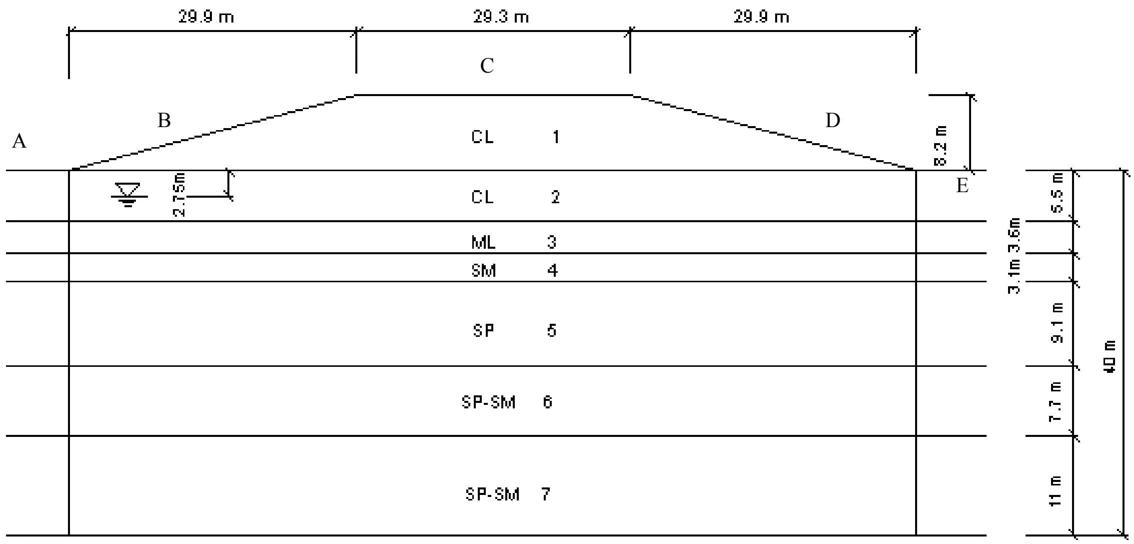

Figure 5. Embankment profile including foundation soils

Figure 6 shows the horizontal and vertical displacements along the embankment surface. The maximum horizontal displacements in the positive x direction occurred at location E, and in the negative direction they occurred at location A. The maximum horizontal displacements in the positive x direction range from 0 to 0.8 m. The maximum negative horizontal displacement was -0.35 m for M7.0. The vertical displacements are symmetrical along the middle of the embankment. The maximum settlements occurred at locations B and D, ranging from 0.15 to 0.35 m. Heave happened in front of the toe. It can be observed from Figure 6 that the slope slide along a surface and the maximum deformation occurred near the toe of the slope.

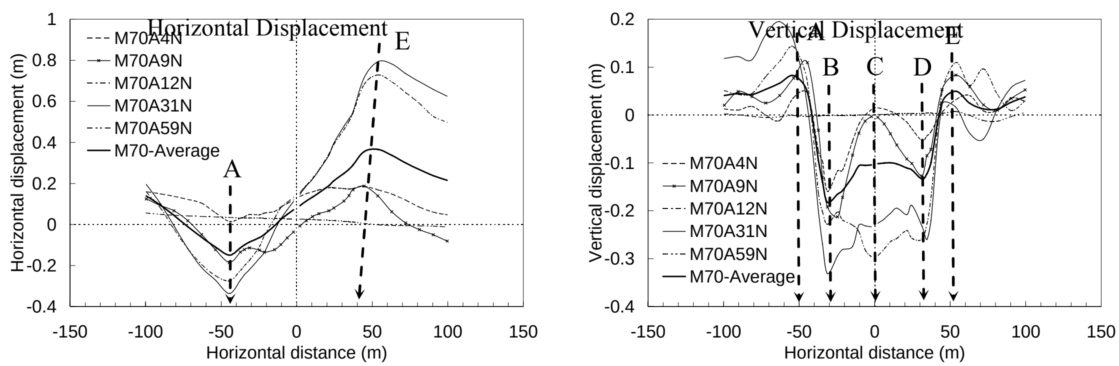

Figure 6. Displacement along embankment surface

Summary

A modified hyperbolic model was developed and implemented into FLAC. The numerical model was calibrated against the 1971 failure of the Upper San Fernando Dam. This modified hyperbolic model can provide good estimate for the earthtuakeinduced deformation. It was then applied to study the permanent deformation of the approach embankment at Bridge Site A1466. The results showed that large deformation would occur in the embankment during an earthquake with a magnitude larger than M7.0. The maximum displacements would take place at the toe of the embankment, and heave would occur in front of the toe of embankment.

References

Beaty, M.H. (2001), A synthesized approach for estimating liquefaction-induced displacements of geotechnical structures, Ph.D. Dissertation, University of British Columbia.

Byrne, P.M. (1991). "A cyclic shear volume – coupling and porewater pressure model for sand." *Second International Conference on Recent Advances in Geotechnical Earthquake Engineering and Soil Dynamics*, St. Louis, Missouri, Report 1.24, Vol.1, March, pp. 47-56

Finn, W.D.L., Yogendrakumar, M., and Yoshida, N. (1986). *TARA-3: A Program to Compute the Response of 2-D Embankment and Soil-structure Interaction Systems to Seismic Loadings*, Department of Civil Engineering, University of British Columbia, Vancouver.

Finn, W.D.L., Sasaji, Y., Wu, G., and Thavaraj, T. (1999) "Stability of flood protection dikes with potentially liquefiable foundations: analysis and screening criterion." *Proceedings of 13th Annual Vancouver Geotechnical Society Symposium*, Vancouver, B.C., 47-54.

Harder, L.F. and Seed, H.B. (1986). "Determination of penetration resistance for coarse-grained soils using the Becker Hammer Drill." Report UCB/EERC-86/06, Earthquake Engineering Research Center, University of California, Berkeley, 126 pp.

Itasca Consulting Group, Inc., FLAC-Fast Lagrangian Analysis of Continua. Version 4.0. Itasca Consulting Group, Inc., Minneapolis, Minn, 2002.

Lin, J.-S. &Hynes, M.-E. (1998). Seismic Discontinuous Deformation Analysis. In P.

Liu, W.X. (2005), Seismic site response of deep soil and embankments in the New Madrid Seismic Zone, Ph.D. Dissertation, University of Missouri-Rolla.

Makdisi and Seed (1978). "Simplified procedure for estimation dam and embankment earthquake-induced deformations." *Journal of the Geotechnical Engineering Division*, ASCE, 104(GT7), 849-867.

Martin, G.R., Finn, W.D.L., and Seed, H.B. (1975). “Fundamentals of liquefaction under cyclic loading.” *Journal of the Geotechnical Engineering Division*, ASCE, 101(GT5), 423-438.

Masing, G. (1926). “Eigenshannungen und verestigung beim messing.” *Proceedings of the Second International Congress of Applied Mechanics.*

Muraleetharan, K.K., Mish, K.D., Yogachandran, C., and Arulanandan, K. (1988). *DYSAC2: dynamic soil analysis code for 2-dimensional problems,* Department of Civil Engineering, University of California, Davis, California.

Newmark, N. (1965). “Effects of earthquakes on dams and embankments.” *Geotechnique*, 15(2), 139-160

Prévost, J.H. (1981). *DYNAFLOW: a nonlinear transient finite element analysis program,* Department of Civil Engineering, Princeton University, Princeton, N.J.

Rathje, E.M. & Bray, J.D. (1999). “An examination of simplified earthquake-induced displacement procedures for earth structures.” *Canadian Geotechnical journal*, 36(1), 72-87

Seed, H.B. and Idriss, I.M. (1970). “Soil moduli and damping factors for dynamic response analysis.” *Report EERC 70-10*, Earthquake Engineering Research Center, University of California, Berkeley.

Seed, H.B., Lee, K.L., Idriss, I.M., and Makdisi, F. (1973). “Analysis of the slides in the San Fernando dams during the earthquake of February 9, 1971.” Report No. EERC 73-2, University of California, Berkeley.

Seed, H. B., P. P. Martin and J. Lysmer.(1975). The generation and dissipation of pore water pressures during soil liquefaction, University of California, Berkeley, Earthquake Engineering Research Center, NSF Report PB-252 648, August.

Serff, N., Seed, H.B., Makdisi, F.I., and Chang, C.Y. (1976). *Earthquake induced deformation of earth dams.* UCB/ERRC-76/04, Earthquake Engineering research Center, University of California, Berkeley, Calif.

Wu, G. (1998). *VERSAT: a computer program for static and dynamic 2-dimensional finite element analysis of continua*, release 98, Wutec Geotechnical International, Vancouver, B.C.

Wu, G. (2001). “Earthquake-induced deformation analysis of the Upper San Fernando Dam under the 1971 San Fernando Earthquake.” *Canadian Geotechnical Journal*, 38(1), 1-15

Zienkiewicz, O.C., Chan, A.H.C., Pastor, M., Paul, D.K., and Shiomi, T. (1990a). "Static and dynamic behavior of soils: a rational approach to quantitative solutions, Part I: Fully saturated problems." *Proceedings of the Royal Society of London*, Series A, 429: 285-309

Zienkiewicz, O.C., Xie, Y.M., Schrefler, B.A., Ledesma, A., and Bicanic, N. (1990b). "Static and dynamic behavior of soils: a rational approach to quantitative solutions. Part II: Semi-saturated problems." *Proceedings of the Royal Society of London*, Series A, 429: 311-321.

Acknowledgments.

Thanks to Dr. Peter Byrne and Dr. Michael Beaty for providing input ground motion for the San Fernando dams to the 1971 San Fernando earthquake.